Suppmentary Table 1. Epitope specific dystrophin antibodies

Name	Epitope	Dilution	Source
Dys-3*	Hinge 1	1:20	Novocastra
Dys-1	Repeats 6-8	1:100	Novocastra
Mandys8	Repeats 11	1:200	Sigma
Mandys102	Repeats 16	1:20	Dr. Glenn Morris
Manex 44A	Repeats 17	1:500	Dr. Glenn Morris
Manex 46B	Repeats 18	1:1,000	Dr. Glenn Morris
Manex 50	Hinge 3	1:2,000	Dr. Glenn Morris
Dys-2	C-terminus	1:30	Novocastra

*, Dys-3 only recognizes human dystrophin

MU# 36612-RG-1 Revision 2

Supplementary Figure Legends

Supplementary Figure 1. Controls for nNOS immunofluorescence staining and *in situ* nNOS activity staining. Serial sections of the TA muscles were evaluated for dystrophin and nNOS expression as well as for nNOS activity. Top panel, representative photomicrographs from BL10 mice. Bottom panel, representative photomicrographs from nNOS knockout mice. Dystrophin was recognized with an R17 specific antibody and a C-terminus specific antibody. Inverted black-and-white images of immunofluorescence (IF) staining are presented. Asterisk denotes the same myofiber in each panel. Scale bar, 50 μm.

Supplementary Figure 2. Adding four spectrin-like repeats (R16 to R19) to the ΔH2-R19 mini-dystrophin gene restores nNOS to the sarcolemma. Representative double immunofluorescence staining photomicrographs with the Dys-3 antibody (a human dystrophin hinge 1 specific antibody, Hum Dys) and an nNOS antibody. The full-length gene or different synthetic minigene expression plasmids were transfected into the tibialis anterior (TA) muscle in 2-month-old *mdx* mice. Immunostaining was performed at two weeks after transfection. In merged images, the constructs that restored nNOS are in yellow color. The constructs that did not restore nNOS are in red color. Revertant fibers are in green color. Scale bar, 50 μm.

Supplementary Figure 3. Epitope mapping of dystrophin plasmids and correlation with sarcolemmal nNOS expression. Inverted black-and-white images are double immunofluorescence (IF) staining on serial muscle sections with an antibody against nNOS and

the indicated epitope-specific antibodies that recognize different regions of dystrophin, respectively. Asterisk, the H1 antibody only reacts with human dystrophin. Color panels (separated by a vertical dotted line in each panel) are the merged image of R16 and nNOS double immunostaining (top) and *in situ* nNOS activity staining (bottom). **A,** Representative images from the full-length human dystrophin plasmid transfected *mdx* TA muscle. **B,** Representative images from the ΔH2-R19 mini-dystrophin plasmid transfected *mdx* TA muscle. **C,** Representative images from the ΔH2-R17 mini-dystrophin plasmid transfected *mdx* TA muscle. **D,** Representative images from the ΔH2-R16 mini-dystrophin plasmid transfected *mdx* TA muscle. Scale bar applies to all panels. Scale bar, 20 μm.

Supplementary Figure 4. The R16/17, but not the R16, containing microgene restores sarcolemmal nNOS. Representative serial immunostaining and nNOS activity staining photomicrographs in *mdx* muscles infected with AAV microgene vectors (N = 4 for each vector). Top panel, a microgene missing R17 did not restore nNOS to the sarcolemma. Asterisk, AAV transduced myofiber; Cross, a revertant myofiber. Bottom panel, a microgene with both R16 and R17 recruited nNOS to the sarcolemma. Double cross, an AAV transduced myofiber. Square denotes the same myofiber in serial sections. Scale bar, 50 μm.

Supplementary Figure 5. Confirmation of transgene expression at the time of histology study. Serial sections shown in Figure 3A were evaluated by immunofluorescence staining using antibodies against nNOS and different regions of dystrophin. Yellow squares mark the same myofibers in different panels. Scale bar, 100 μm.

Supplementary Figure 6. Systemic delivery of AAV-9 AV.CMV.ΔR2-15/ΔR18-23/ΔC in newborn *mdx4cv* mice improves skeletal muscle specific force and reduces serum CK levels. Specific force of the extensor digitorium longus (EDL) muscle (left panel) and serum CK levels (right panel) were examined at three months after AAV injection. Age and sex-matched BL6 and *mdx4cv* mice were included as controls. Asterisk, the results from BL6 mice were significantly better than those from *mdx4cv* mice ($p \leq 0.0004$). Cross, the specific force from AAV infected *mdx4cv* mice were significantly higher than those of uninfected *mdx4cv* mice under all stimulation frequencies ($p \leq 0.0004$) but significantly lower than those of BL6 mice under stimulation frequencies of 80, 120 and 150 Hz ($p \leq 0.004$). At the 50 Hz stimulation frequency, there was no statistical difference between AAV infected *mdx4cv* mice and BL6 mice ($p = 0.093$). Double cross, the CK value from AAV infected *mdx4cv* mice was significantly lower than that of uninfected *mdx4cv* mice ($p = 0.003$) but was not statistically different from that of BL6 ($p = 0.193$). Sample size for the left panel, N = 7 for BL6; N = 6 for uninfected *mdx4cv*; N = 6 for AV.CMV.ΔR2-15/ΔR18-23/ΔC infected *mdx4cv* mice. Sample size for the right panel, N = 5 for BL6; N = 10 for uninfected *mdx4cv*; N = 14 for AV.CMV.ΔR2-15/ΔR18-23/ΔC infected *mdx4cv* mice.

Supplementary Figure 7. Norepinephrine (NE)-mediated vasoconstrictor responses in transgene-negative littermates. ΔH2-R15 minigene transgenic mice were backcrossed with mdx mice for five generations. Transgene-negative offspring from the last backcross were used in this study. Femoral vascular conductance was measured in resting and contracting hindlimbs after two independent doses of norepinephrine administration. AUC, area under the curve in arbitrary units. N = 3.

Supplementary Figure 8. Norepinephrine (NE)-mediated vasoconstrictor responses in transgenic *mdx4cv* mice. Femoral vascular conductance was measured in resting and contracting hindlimbs in 6 to 11-m-old male HSA.ΔH2-R15 and HSA.ΔH2-R19 transgenic *mdx4cv* mice after one dose of non-epinephrine administration (4 to 10 ng in 2 to 5 μl). AUC, area under the curve in arbitrary units. N = 3 for each group. Asterisk, significantly different from resting.

Supplementary Figure 9. Treadmill performance in BL10, mdx and ΔR4-23 micro-dystrophin transgenic mdx mice (all on the BL10 background). **A,** running distance; **B,** body weight normalized running distance; **C,** relative running distance change comparing with that of the day 1. BL10 mice have normal sarcolemmal nNOS and their running performance improved continuously over the 10-day period. Mdx mice showed moderate increase in the first 4 days and then leveled off. ΔR4-23 micro-dystrophin transgenic mdx mice express a functional microgene in muscle but sarcolemmal nNOS is not restored. Consistent with our previous report (Harper et al Nature Medicine 8:253-261, 2002), microgene transgenic mice run better than BL10 mice initially. Their running performance was enhanced in the first 3 days but leveled off thereafter. By day 9, transgenic mice performance dropped below that of BL10 (panels A and B). Asterisk, values in the BL10 group are significantly higher than those in the mdx group and the ΔR4-23 microgene transgenic group.

Supplementary Figure 10. Histopathology and dystrophin expression in the limb muscles of minigene transgenic mdx mice following eight-day treadmill running. A, Representative

HE staining. High magnification images of the boxed areas are shown in Figure 7 in the manuscript. Arrows, regenerating myofibers seen in ΔH2-R19 transgenic mice. **B,** Representative immunofluorescence staining with human dystrophin hinge 1 specific antibody. High magnification images of the boxed areas are shown in Figures 7B and 7C in the manuscript. Scale bar, 50 μm.

Lai et al 2008 R2
Supplementary Figure 1

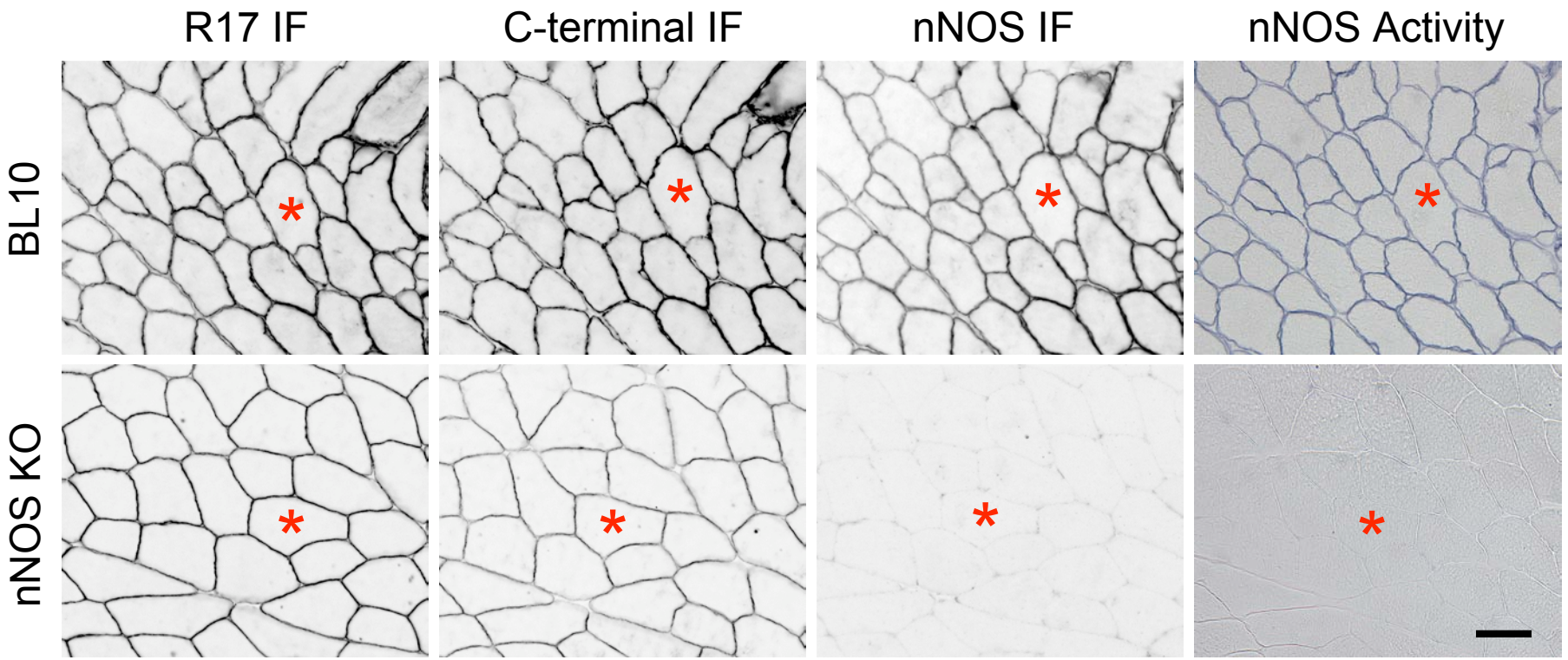

Lai et al 2008 R2
Supplementary Figure 2

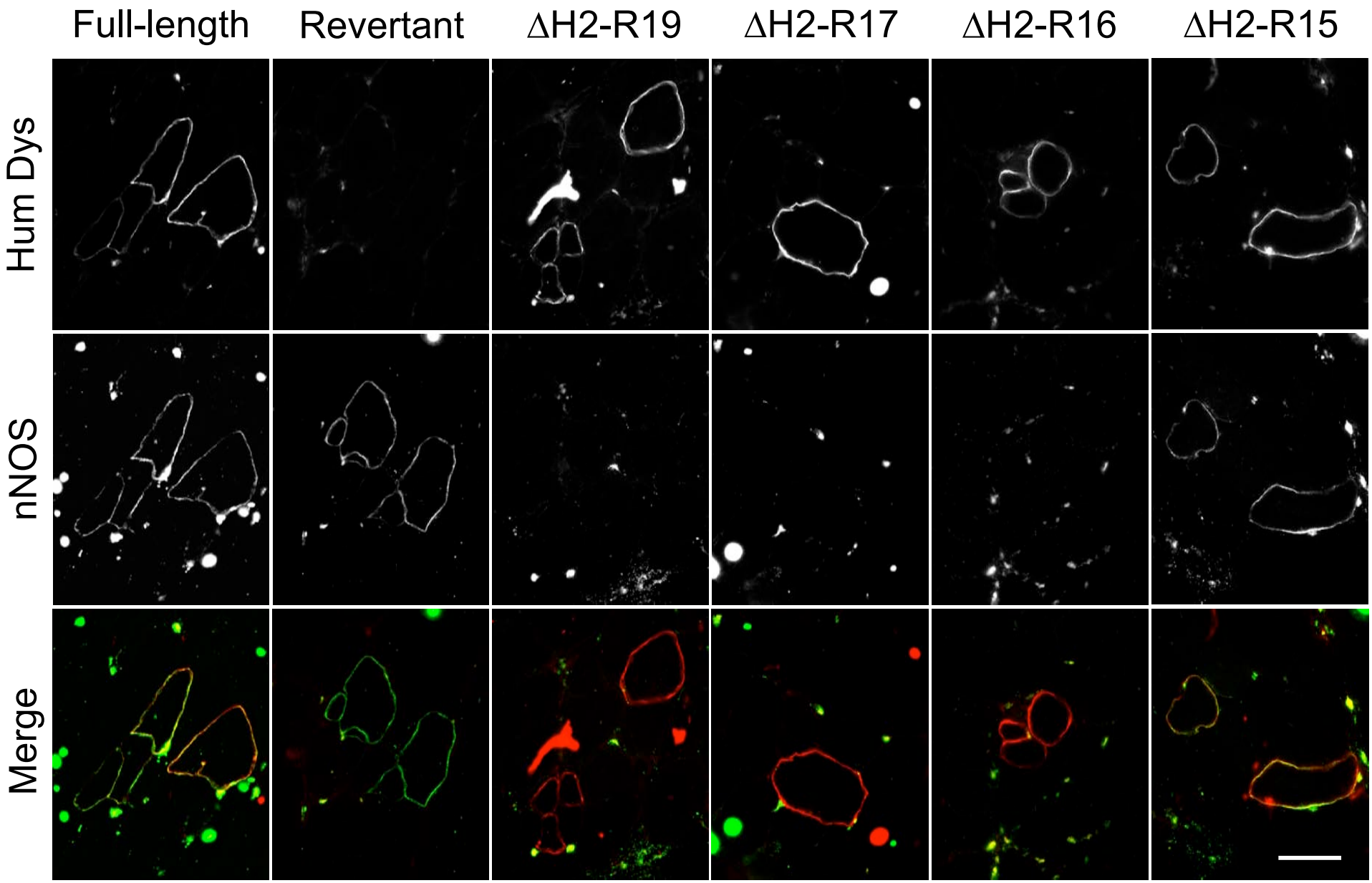

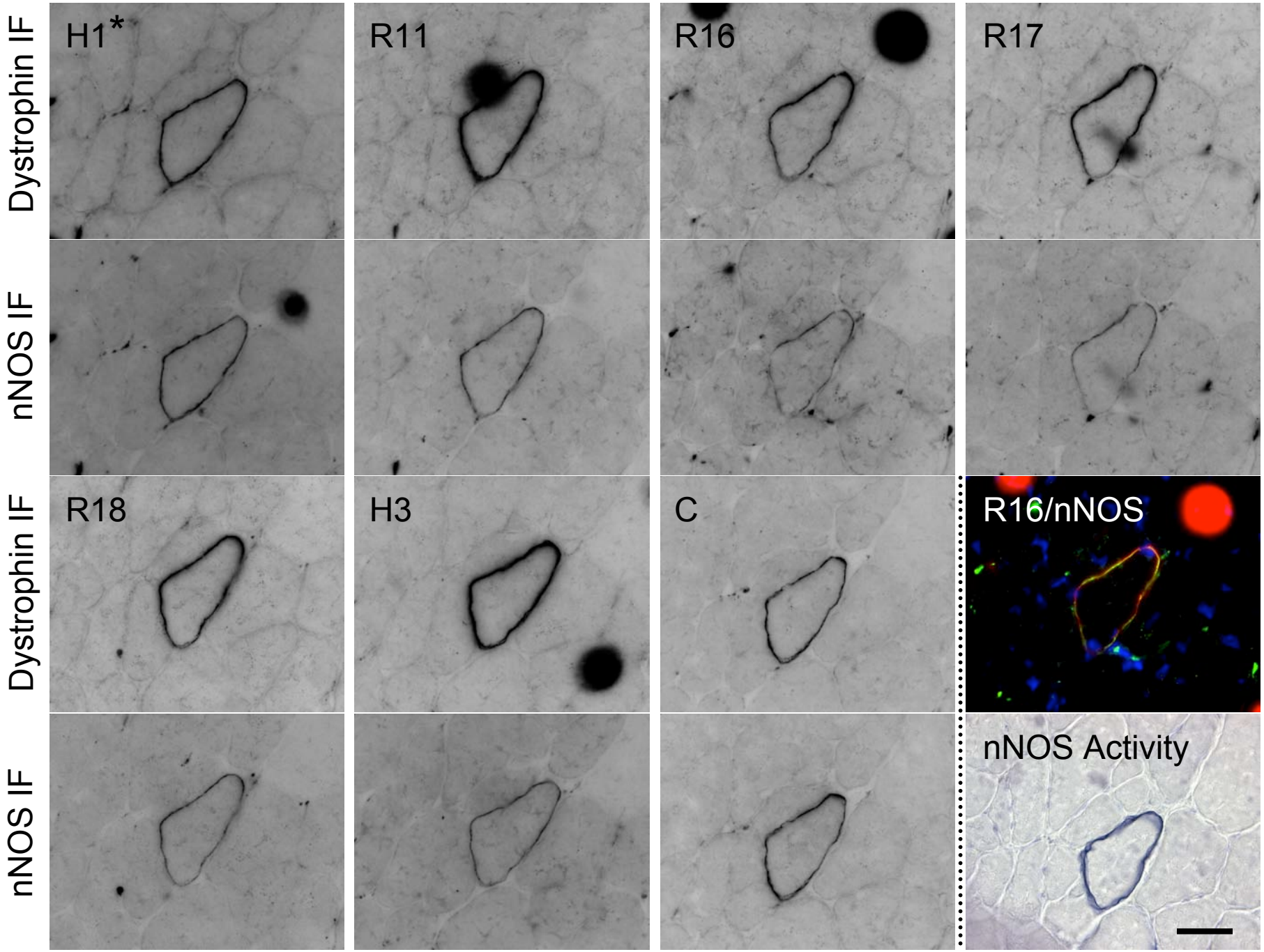
A
(Full-length human dystrophin)
Dystrophin IF
nNOS IF
Dystrophin IF
nNOS IF
H1*
R11
R16
R17
R18
H3
C
R16/nNOS
nNOS Activity

B (ΔH2-R19 mini-dystrophin)

Lai et al 2008 R2; Supplementary Figure 3B

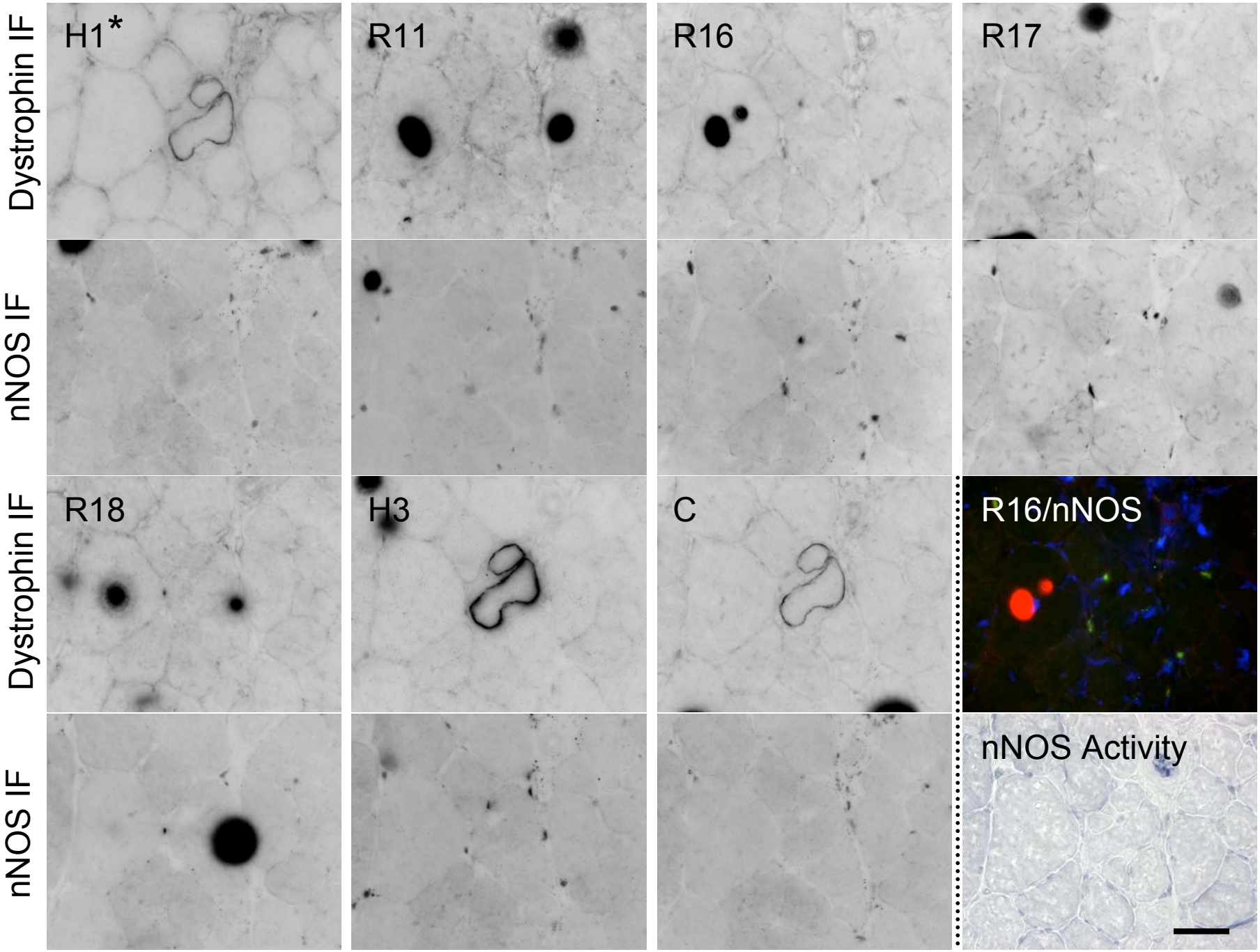

C (ΔH2-R17 mini-dystrophin)

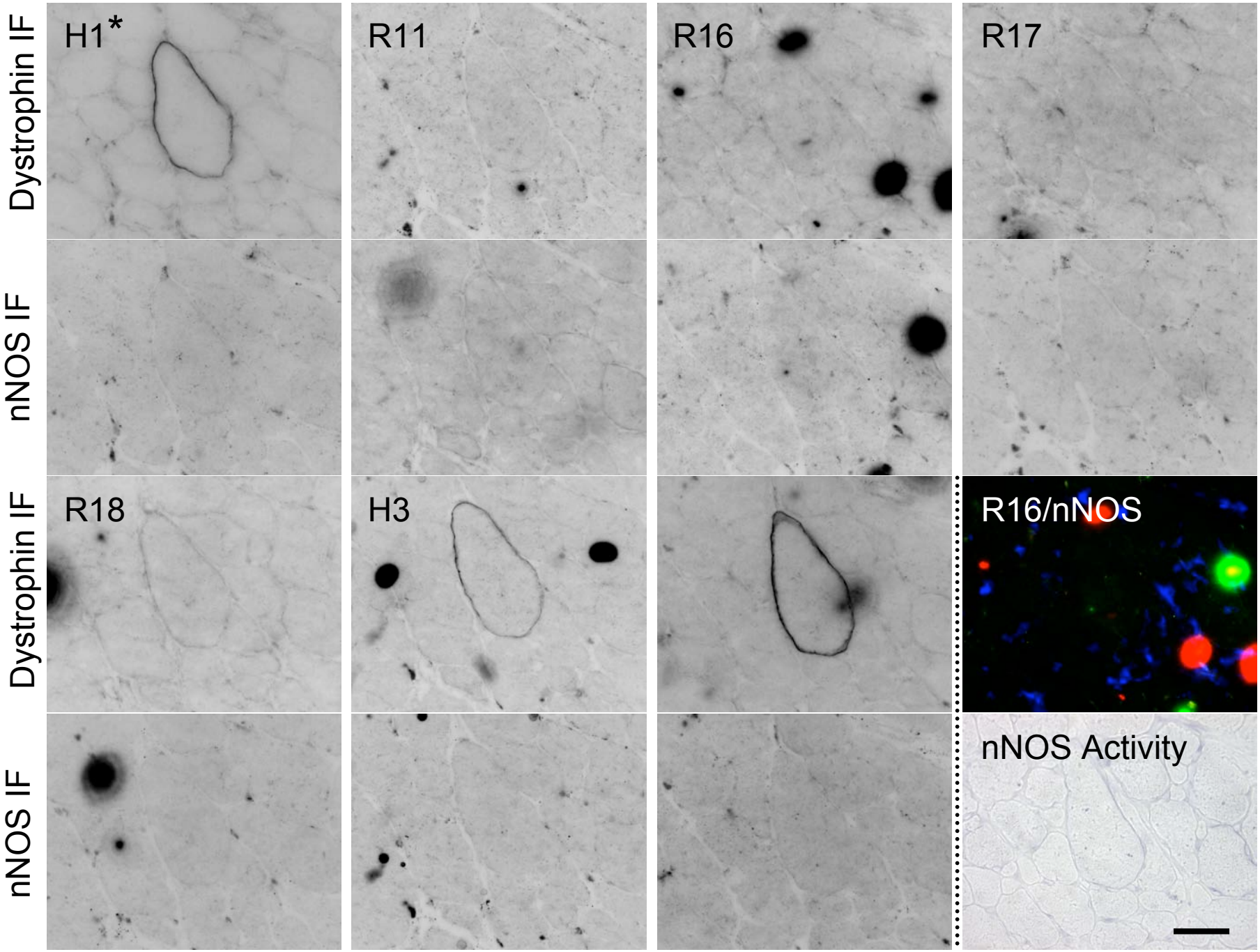

D (ΔH2-R16 mini-dystrophin)

Lai et al 2008 R2; Supplementary Figure 3D

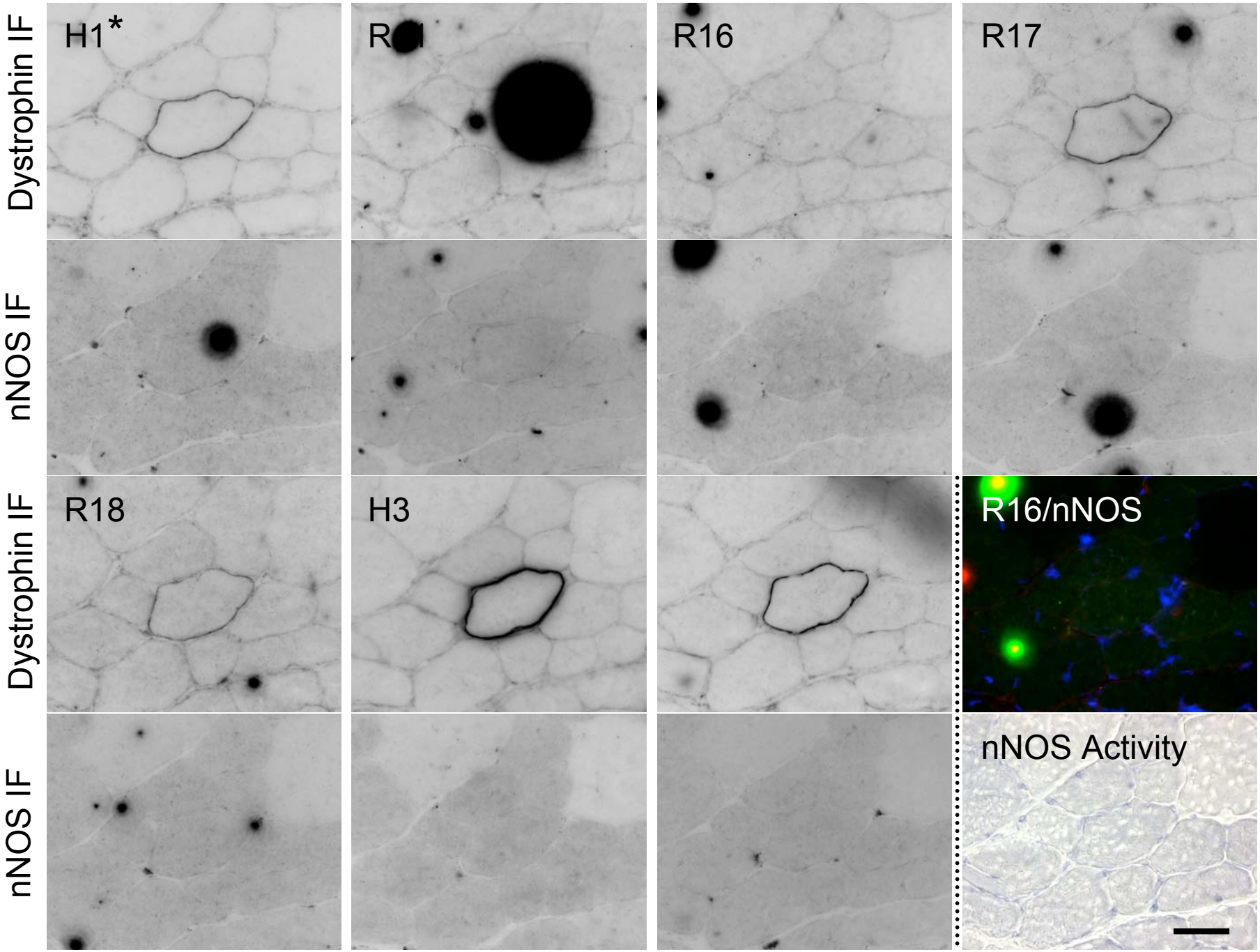

Lai et al 2008 R2
Supplementary Figure 4

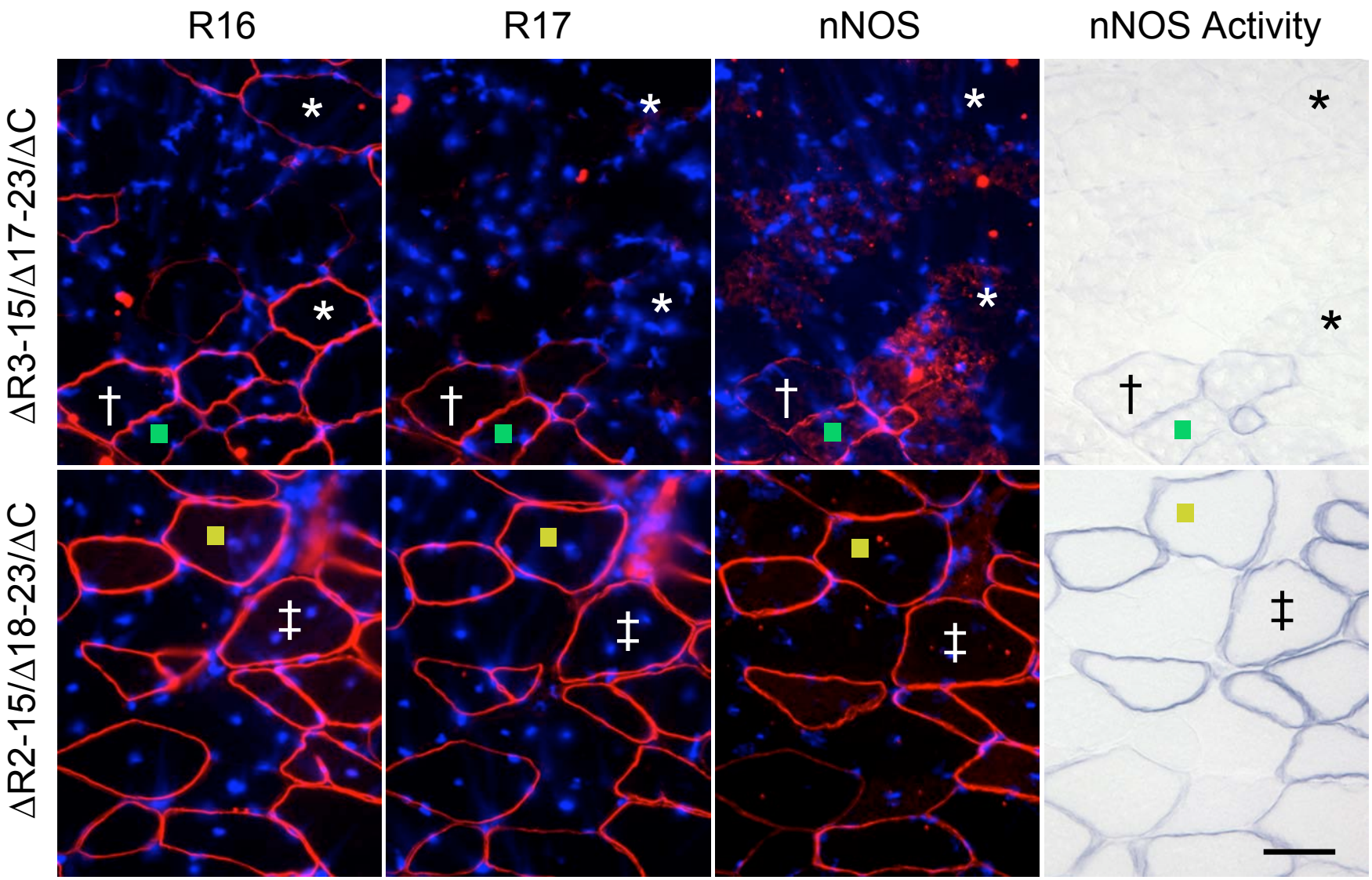

Lai et al 2008 R2
Supplementary Figure 5

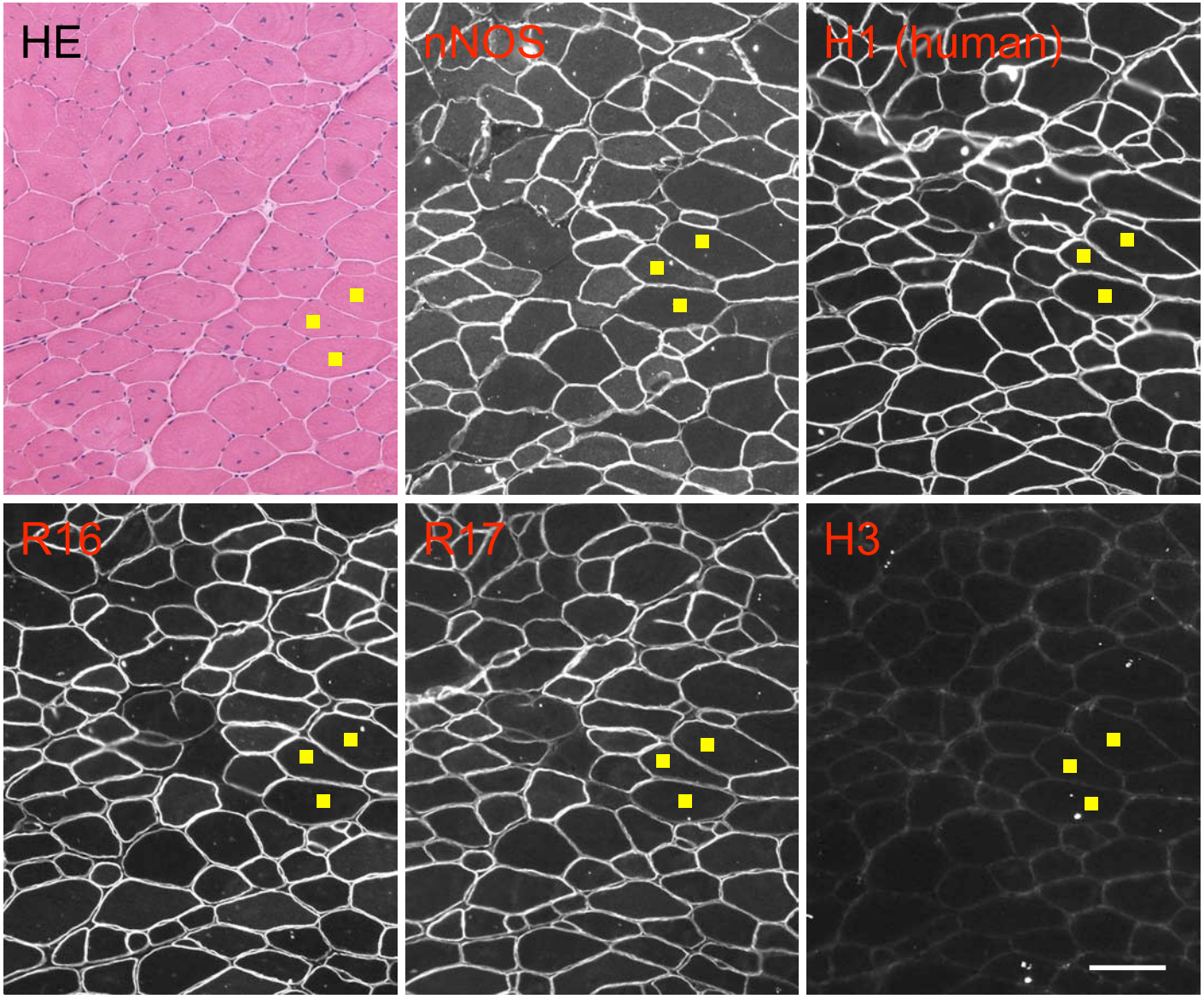

Lai et al 2008 R2
Supplementary Figure 6

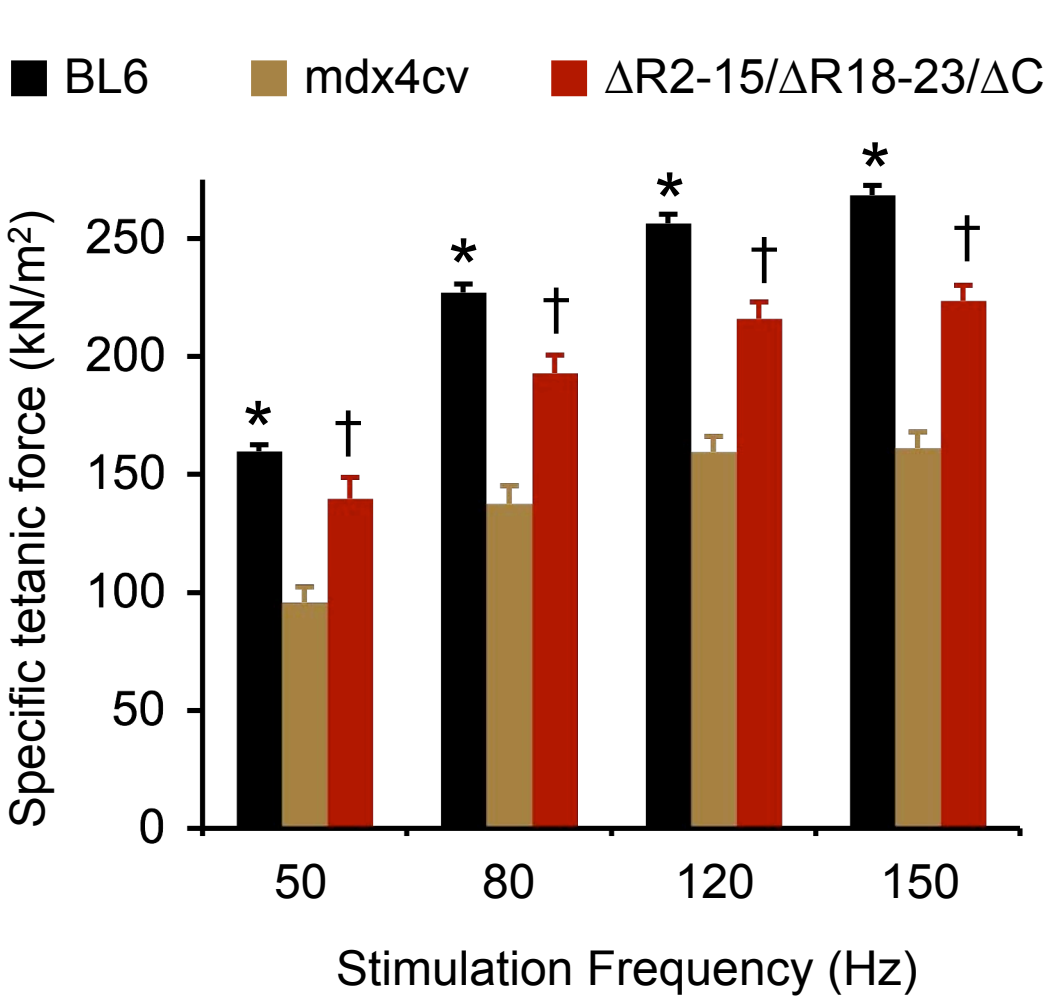

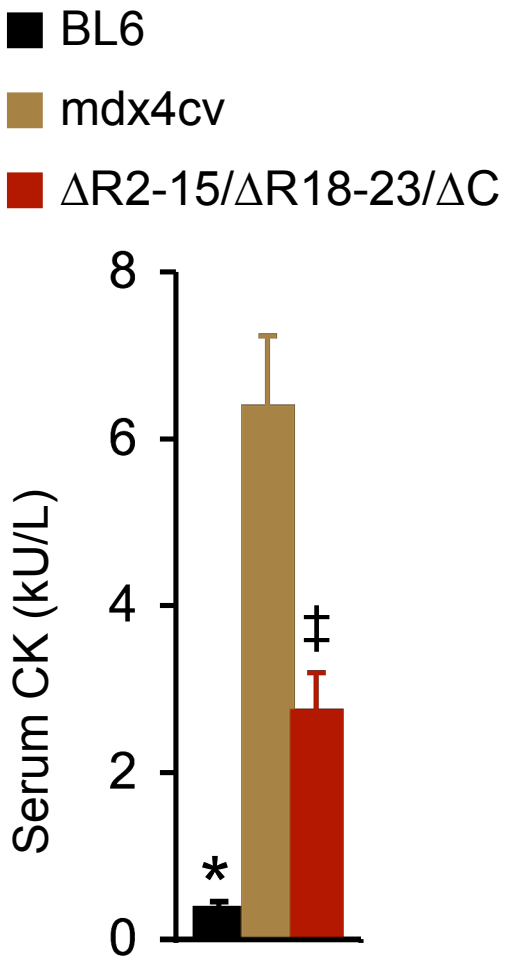

Lai et al 2008
Supplementary Figure 7

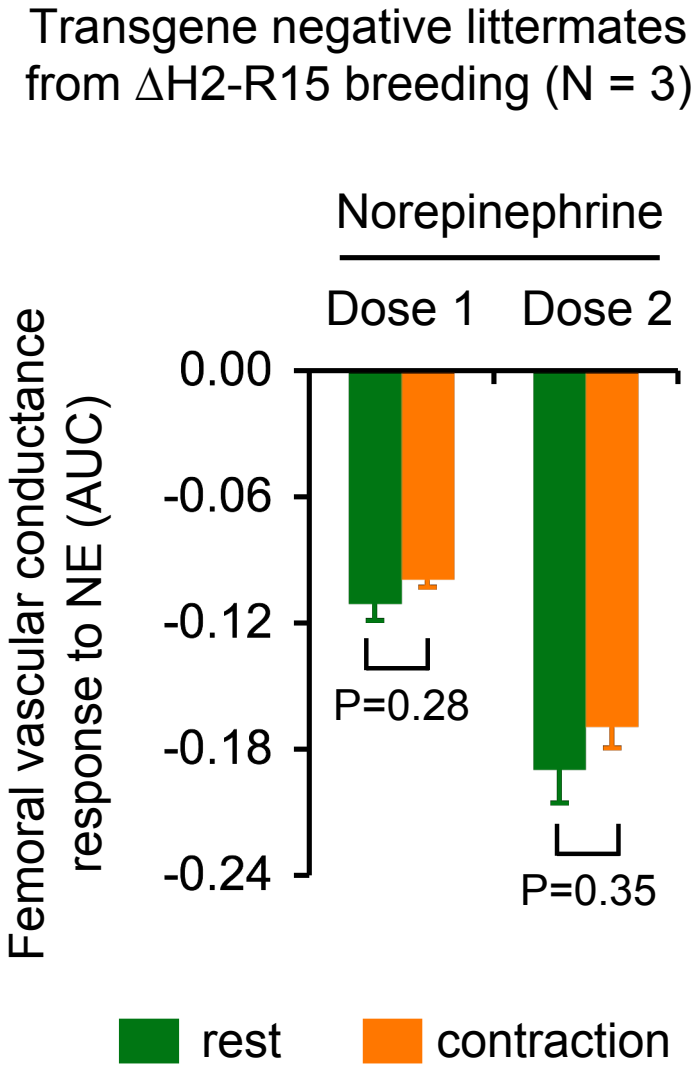

Lai et al 2008 R2
Supplementary Figure 8

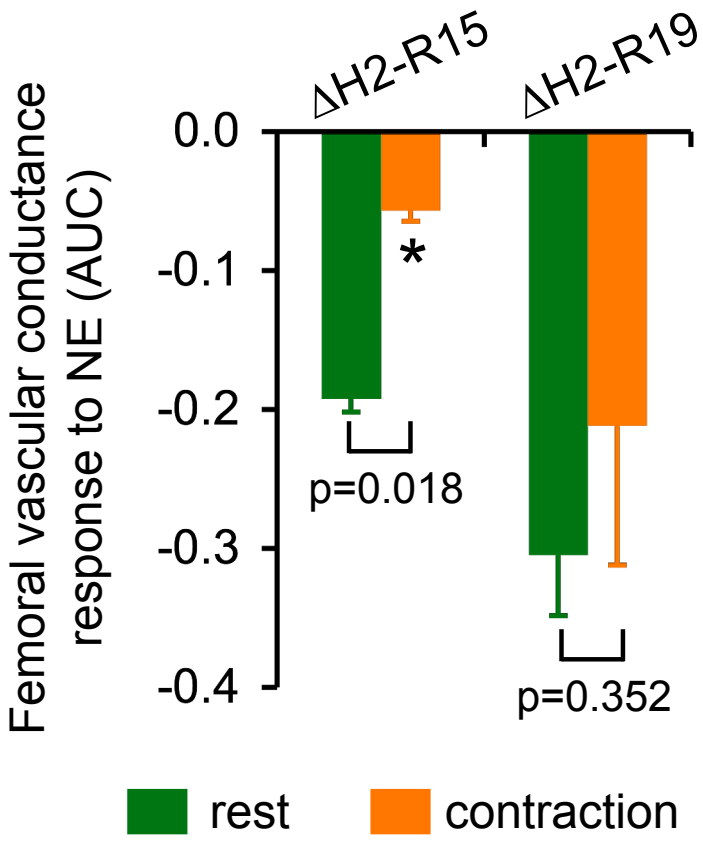

Lai et al 2008 R2
Revised Supplementary Figure 9

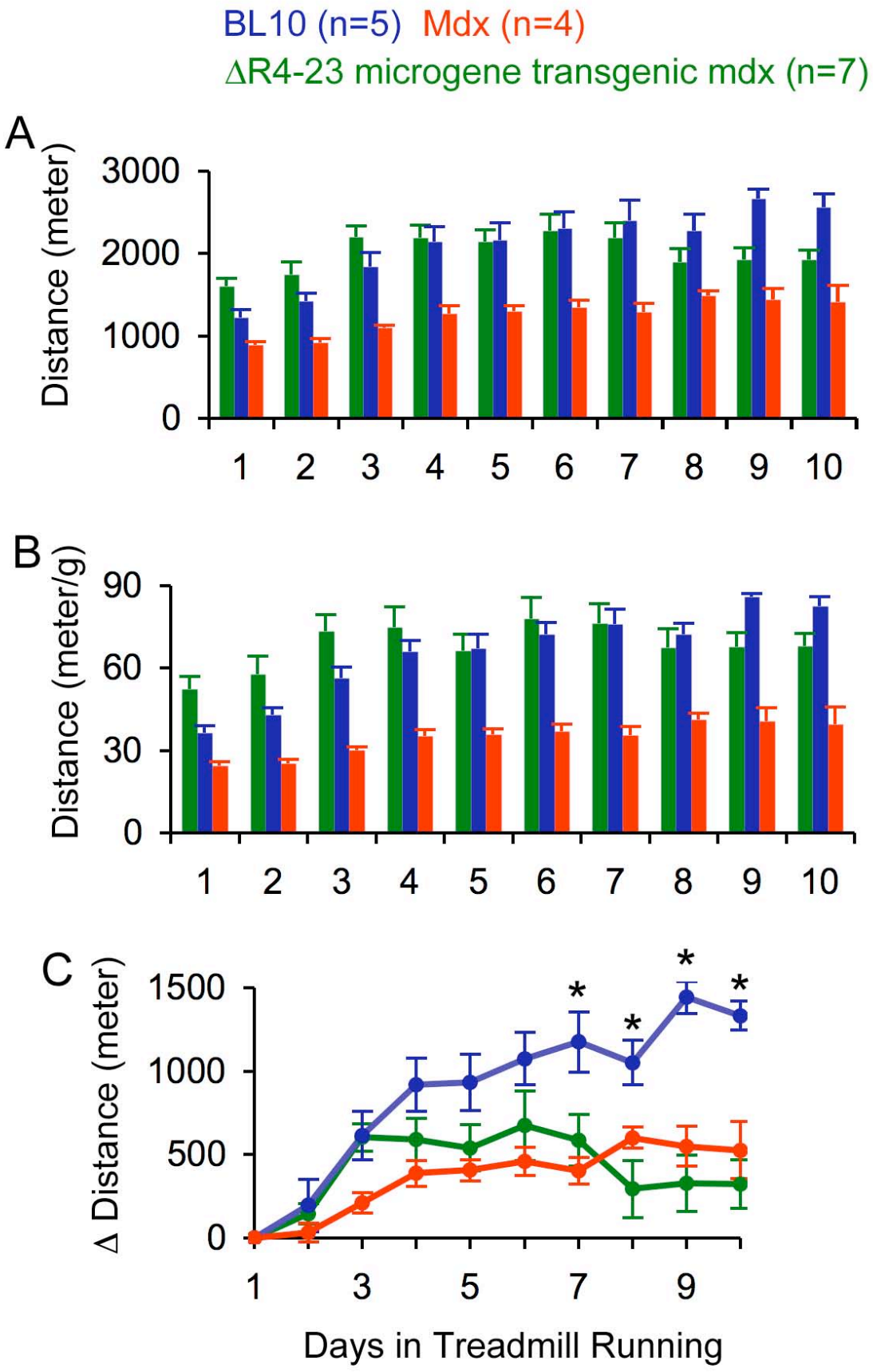

Lai et al 2008 R2
Supplementary Figure 10A

A

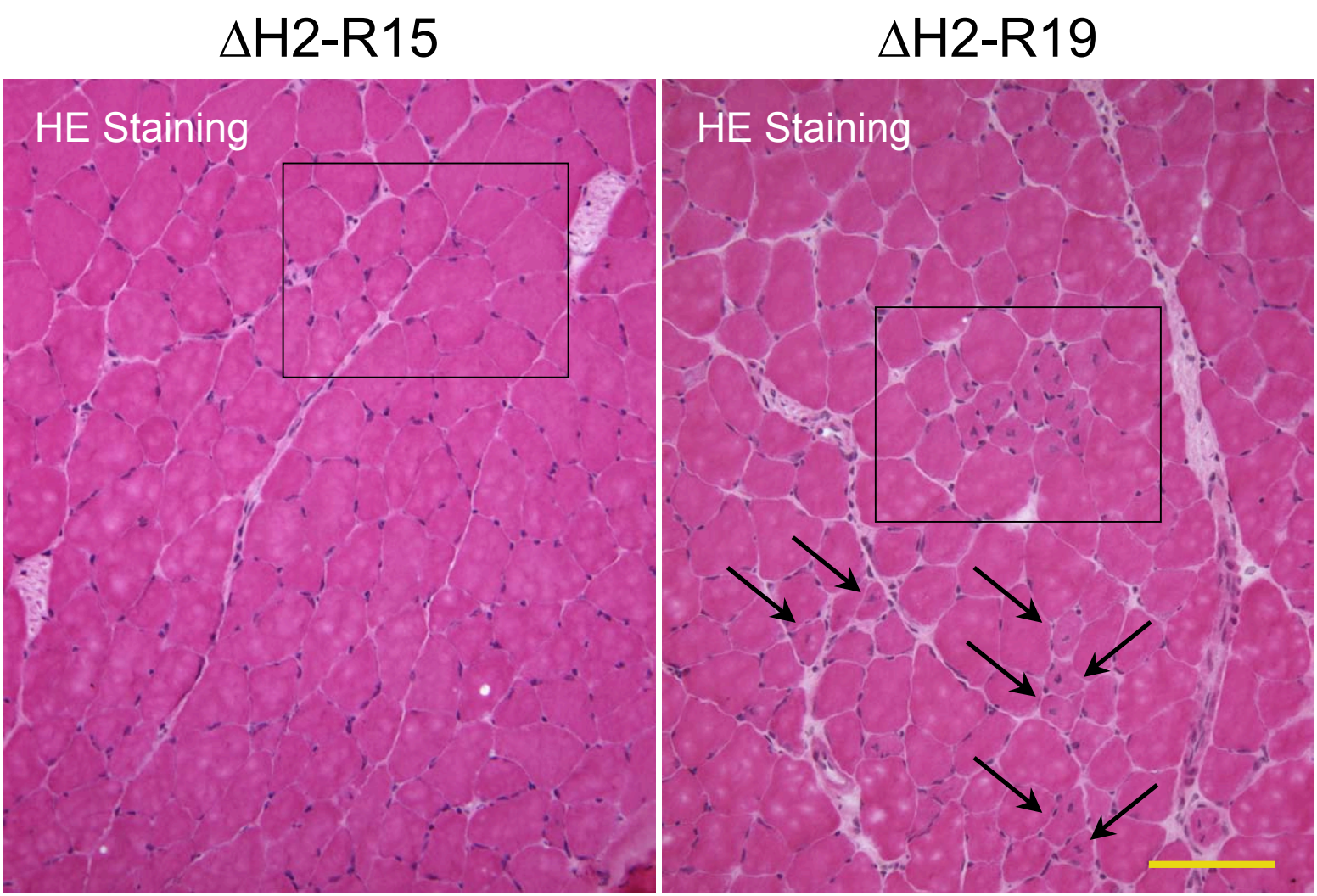

Lai et al 2008 R2
Supplementary Figure 10B

B